Three-Dimensional Finite Element Analysis of a Novel Silicon Based Tactile Sensor with Elastic Cover

Chunxin Gu, Weiting Liu(✉), and Xin Fu

The State Key Lab of Fluid Power Transmission and Control,
Zhejiang University, Hangzhou 310027, China
{cxgu,liuwt,xfu}@zju.edu.cn

Abstract. Tactile sensors are indispensable in robotic or prosthetic hands, which are normally covered with or embedded in soft materials. A novel tactile sensor with the structure of combining an elastic steel sheet and a piezoresistive gauge has been developed in the previous work. To better understand the mechanical effects of soft cover on this sensor, a three-dimensional finite element model (FEM), which is based on linear elastic behavior, is established. As usual, polydimethylsiloxane (PDMS) is adopted as the soft cover material. The results indicate that though soft cover diffusion of mechanical signals still exists, the steel sheet strengthens the measuring ability and at the same time lowers the density of sensing units to identify the single indentation location.

Keywords: Tactile sensor · Steel sheet · Soft cover · FEM · PDMS

1 Introduction

Like human skin, the soft cover for artificial tactile sensing plays a significant role in protecting the subsurface sensors from damage or for better hand-to-object contact. However, the skin-like soft cover blurs the signals that are transmitted to the embedded sensor due to its mechanical properties, which makes the measurement of the whole tactile system less reliable.

The existing researches have mainly focused on the transducers; only in a few works, the cover effects have been studied. R. S. Fearing etc. in [1] used a simple linear elastic model to predict strains beneath a compliant skin for a finger touching a knife edge, a corner, and a flat surface; M. Shimojo in [2] analyzed the mechanical spatial filtering effect of an elastic cover for different types of cover materials; P. Tiezzi etc. in [3] performed a series of experimental tests to analyze the influence of the thickness of the compliant layer on the resultant fingertip stiffness; J. Z. Wu etc. in [4] analyzed the contact interactions between the fingertips and objects with different curvatures via a 2D finite element fingertip model and in [5] predicted the time-dependent force responses of the fingertip via a 3D model; J.-J. Cabibihan etc. in [6] used a FEM based on viscoelastic and hyperelastic behavior to determine the effects of various thickness of the synthetic skin on the pressure distribution. All these works are based on the assumption that the embedded sensors are small and dependent which will not interfere with the mechanical behavior of the soft cover. However, because the tactile sensor we previously

H. Liu et al. (Eds.): ICIRA 2015, Part I, LNAI 9244, pp. 402–409, 2015.
DOI: 10.1007/978-3-319-22879-2_37

developed in [7] has the novel structure as the combination of the steel sheet and silicon gauge which makes the detecting value largely depend on the deflection of the steel sheet, the coupling effects between the steel sheet and the soft cover should be taken into consideration when analyzing the mechanical properties of the whole sensor.

In this paper, a three-dimensional FEM of a tactile sensor covered with a PDMS layer is proposed, which treats the PDMS material as linear elastic to simplify the modelling. And the function of the steel sheet is analyzed in aspects of valid mechanical signals transmission and single indentation location identification.

2 Sensor Design and Fabrication

The sensor consists of four parts as illustrated in Fig. 1, the PDMS layer, the steel sheet, the silicon gauges and the flexible printed circuit board (FPCB). The origin of coordinate is set on the center of the upper surface of the steel sheet. A tactile sensor with one silicon gauge but without PDMS layer has been developed, and more details about the structure of the sensor are available in the previous work [7]. To fit the finger of the artificial hand, the dimensions of the developed sensor are set as: L1, 15mm; L2, 15mm; H1, 0.3mm. The planar PDMS layer is glued to the steel sheet, and its bottom surface has the same dimensions as the upper surface of the steel sheet. The thickness H2 of the PDMS layer is set as 2mm which is close to that of human skin (about 521~1977μm[8]). On the bottom surface, three silicon gauges numbered as I, II, III are fixed along the symmetry axis parallel to the x-axis with exact coordinates as (-4, 0, -0.3), (0, 0, -0.3), and (4, 0, -0.3), respectively. At the same time, the valid stretch or compression direction of the silicon gauges should be parallel to the y-axis.

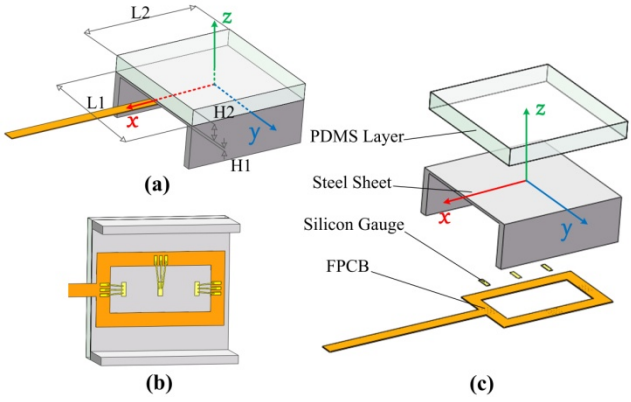

Fig. 1. Sensor structure. (a) A schematic of the sensor structure. (b) A view of the rear surface of the sensor. (c) An exploded view of the sensor (the golden leads are ignored).

The whole tactile system is fabricated easily combining the traditional machining process and the MEMS technology. The steel sheet is polished to guarantee the designed structure after being grinded from a steel block while the silicon gauges are fabricated with an SOI wafer based on the dry etching technology. After that, the silicon

gauges are fixed on the rear surface of the steel sheet by the technology of glass sintering. Around the gauges, the FPCB which is available in the market is glued on the surface. Using the ultrasonic bonding machine, the golden leads are connected to the FPCB and the silicon gauges respectively. Before being glued on the steel sheet, the PDMS layer is made at the mixing ratio of the base polymer to curing agent as 15:1.

3 Methods

By means of the finite element analysis (FEA) simulation tool (ANSYS Workbench 14.5), the mechanical behaviors of the sensor under various indenting conditions are analyzed.

3.1 Finite Element Model

The mechanical properties of the whole tactile system are considered as linear elastic. There are three kinds of materials in the system: PDMS for the soft layer, stainless steel 17-4PH for the steel sheet and structure steel for the indenter whose major mechanical parameters are shown in Table. 1. As the Young's modulus of human finger skin differ greatly due to different races, ages, sexes and measurement methods, a rough range of the Young's modulus is 0.01~20MPa[9] which means that the one we set for the PDMS is about at the mid-level of the range. Considering that the force sensing range for human hand perception is about 0.1N-10N[10], the indenting force is set not larger than 10N. Because the Young's modulus of the steel sheet is large enough compared with the indenting force, the deflection of the steel sheet is very small which indicates only linear elastic properties among consideration. In addition, the PDMS layer could also be assumed as linear elastic when the strain is less than 0.5[11].

Table 1. Material properties used for FEA

Material	Young's modulus	Poisson's ratio
PDMS(15:1)	0.85MPa	0.49
17-4PH	197GPa	0.3
Structure steel	200GPa	0.3

As the steel sheet has two strong braces which are designed to be inserted into the slots of the artificial finger shown in Fig. 2, the boundary condition of the steel sheet can be simplified that the two edges parallel to the x-axis are fixed. The connection of the contact interface between the indenter and the upper surface of the PDMS layer is set as the no separation state, which means there is no gap in the contact interface along the z-direction when the indenting force is applied. The PDMS layer and the steel sheet are modeled as two parts with different materials but belong to the same body, which brings about the continuous state of the geometry structure and the elements division. The elements are divided evenly with the dimension as 0.3mm. The model with elements division is shown in Fig. 2(c).

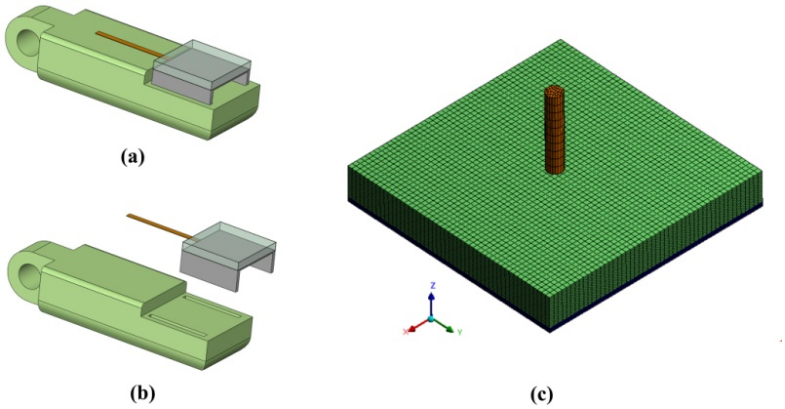

Fig. 2. Schematic of the sensor fixed in the artificial finger & simplified model of the sensor. (a) Assembly of a tactile sensor and an artificial finger. (b) An exploded view of the whole system. (c) The three-dimensional model simplified by removing the two supporting braces and fixing the two opposite edges of the steel sheet (the brown part is the indenter).

3.2 Indenting Conditions

Considering a simple contact condition that a rod indenter is applied on the surface of the soft cover (the PDMS layer here), the mechanical responses are compared with those of the usual tactile systems and the indenting on different locations is also implemented. The diameter of the rod indenter is set as 1mm while the indenting pressure is set as 0.5MPa causing the resultant force as about 0.4N.

1) Effects of the steel sheet deflection: As mentioned before, the steel sheet is the medium layer between the soft cover and the silicon gauges so that the combination of the soft cover and the steel sheet transmits the pressure values on the cover surface to the y-direction normal strain values on the bottom surface for the gauges. Nevertheless, in most tactile systems, the soft cover transmits the normal pressure directly to the sensing units. In other words, we care normal strain for this system but pressure or z-direction normal stress for other usual systems. It is meaningful to compare those two mechanical conditions under the same pressure circumstance. We use the same model introduced before but different support conditions for each cases: the whole bottom surface of the sheet fixed for the usual system (case 1) and two opposite edges fixed for this system (case 2). The indenter is applied at the center of the upper surface of the PDMS layer for both cases.

2) Identification of the indentation location: The rod indenter is applied at different points along the x-axis or lines parallel to the x-axis. The center of the bottom surface of the indenter is located respectively at 0~6mm (space interval as 1mm) from the origin of coordinate along the negative x-axis. After that, the indenting processes are repeated only by changing the y coordinate of the locations from 0 to 2, 4, and 6 respectively. The indentation locations are illustrated in Fig. 5(a) where the green "*"

represents the projection of each indentation location on the upper surface of the steel sheet. During the series of indenting, the y-direction normal strain distribution on the bottom surface of the steel sheet, especially those of the gauge points, is cared about to analyze the relationship between the indentation location and the gauge values.

3.3 Results

1) The z-direction normal stress distribution along the x-axis for case 1 and the y-direction normal strain distribution along the symmetry axis (coordinates: y=0, z=-0.3) on the bottom surface of the steel sheet for case 2 are obtained respectively. In addition, those values are processed further using a simple normalization method that is to make all values divided by that of the center point. The results are shown in Fig. 3, from which we can see that the pressure ratio drops dramatically while the strain ratio changes gently both relative to the distance from the center point. For example, at x=-2 or 2, the pressure ratio has declined to almost zero while the strain ratio still remains at about 0.8. The results indicate that the steel sheet strengthens the diffusion ability of the valid mechanical signal. In the aspect of force location identification, this may not be good for normal tactile sensor array with high density as it adds the complexity of signal coupling. But it will be useful for this kind of sensor because it will lower the demand of high density to determine the single indentation location due to the definite relationship between the values from different gauges.

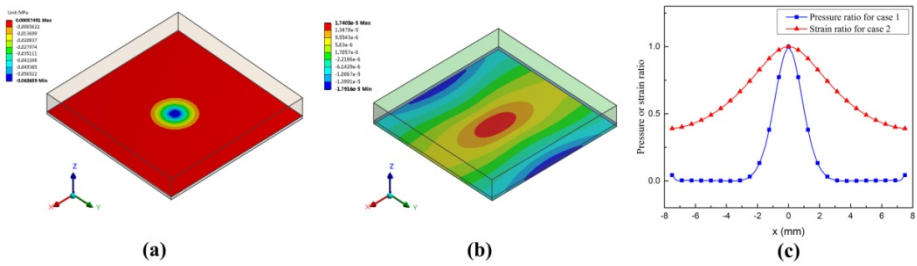

Fig. 3. Pressure or strain distribution for the two cases. (a) Normal pressure distribution on the bottom surface of the PDMS layer for case 1. (b) Y-direction normal strain distribution on the bottom surface of the steel sheet for case 2. (c) Comparison of the trends of the valid mechanical values change along the x-axis between the two cases.

2) For the identification of the indentation location, the y-direction normal strain distribution along the negative x-axis is shown in Fig. 4. The text "xi" in the legend means x coordinate value for each indentation location is "i". As the sensor structure is symmetrical about the center line, the distribution curve will be also symmetrical about the center line if the indentation is added along the positive x-axis. The strain distributions along the other lines whose y coordinate values are 2, 4, and 6 respectively have similar curves, which are not plotted. According to Fig. 4, we can see that when the indentation location changes, the pattern of the distribution curve also changes with the peak point following the indentation location. Besides, each curve inclines slowly when the point is

away from the indentation location, which means that the structure strengthens the expansion of the pressure signal distribution but makes it more definite due to the steel sheet's good linear elasticity and deflection continuity.

Taking advantages of these properties, it is suggested that the single indentation location could be uncovered using the outputs of the three silicon gauges (assuming that the indenter diameter is definite such as 1mm).Therefore, we calculate respectively the ratio of the strain value at x=-4 or 4 (where gauge I and II are) to that at x=0 (where gauge III is) and plot the ratio values relative to the indentation locations in Fig. 5(b). The text "I/II" or "III/II" in the legend represent the ratio of y-direction normal strain value between gauge I and II or between gauge III and II while "yj" means that the trajectory of the indentation points is (y=j, z=0) which is drawn in Fig. 5(a). The right half of the graph is plotted according to the symmetrical property. The combination of the strain ratio values from gauge I/II and III/II are unique at each point of the indentation location regardless of the normal indenting pressure values, making the reverse problem easily solved.

Specifically, the location identification process can be conducted as follows: firstly, compare the two ratio values from gauge I/II and III/II to determine which half space the indentation is in; secondly, for example if in the left half, draw a straight line parallel to the horizontal axis with the value obtained from gauge III/II and find out each intersection point with the calibrated curves; thirdly, compare the value from gauge I/II with the value at the calibrated curve for gauge I/II corresponding to each intersection point to finally determine the exact location. Above all, it is believed that the space revolution will be improved by reducing the space interval in the indenting calibration process.

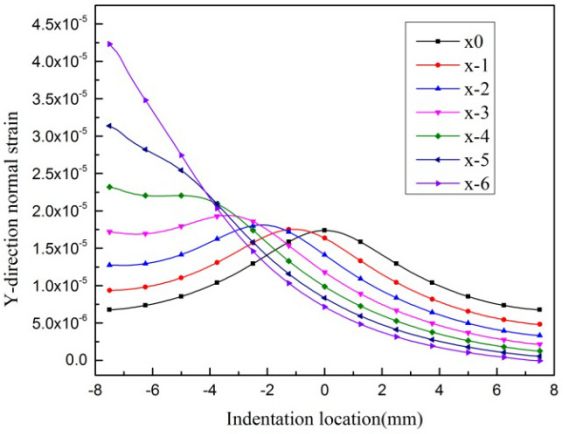

Fig. 4. Y-direction normal strain distribution along the line (y=0, z=-0.3) on the steel sheet under different indentation location conditions.

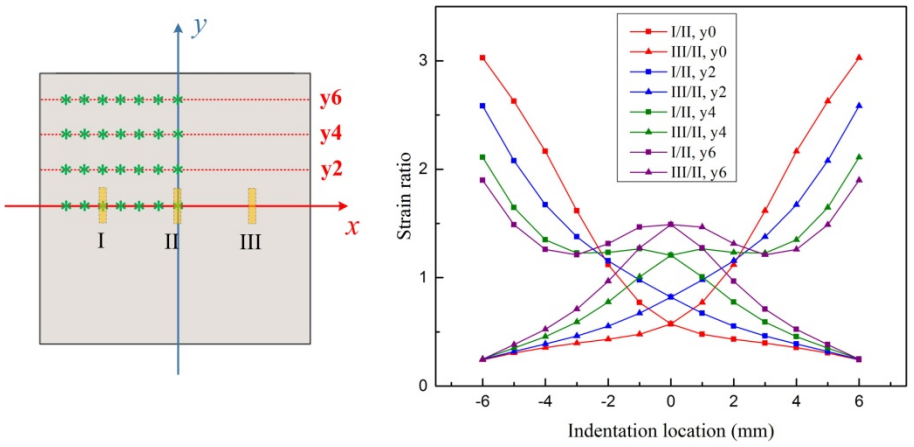

Fig. 5. (a) View of the upper surface of the steel sheet in the z-direction, where the green "*" represents the projection of each indentation location and the yellow rectangle represents the projection of each silicon gauge. (b) Ratio of y-direction normal strain of gauge I or III to that of gauge II along each red line in (a) relative to the indentation location.

4 Conclusions and Future Work

A three-dimensional finite element model for a silicon based tactile sensor covered with an elastic PDMS layer has been proposed. Based on the model, the comparison of mechanical properties between the two systems with or without steel sheet deflection is made, which verifies that the steel sheet strengthens the diffusion of the valid mechanical signal. Moreover, the strain distributions under the indentations on different locations of the elastic cover have been analyzed. The results show that the location of the indenter with certain diameter has unique relationship with the y-direction normal strain values on the exact points where the silicon gauges are fixed, which indicates that the reverse problem about single force location identification will be easily solved even using only three sensing units.

Future work will consist of the integration of the whole tactile system into artificial hand and the experiments of hand-to-object contact to test the performance in the real circumstance.

Acknowledgements. This work is supported by National Basic Research Program (973) of China (No.: 2011CB013303) and the Science Fund for Creative Research Groups of National Natural Science Foundation of China (No.: 51221004).

References

1. Fearing, R.S., Hollerbach, J.M.: Basic solid mechanics for tactile sensing. The International Journal of Robotics Research **4**, 40–54 (1985)
2. Shimojo, M.: Mechanical filtering effect of elastic cover for tactile sensor. IEEE Transactions on Robotics and Automation **13**, 128–132 (1997)
3. Tiezzi, P., Vassura, G.: Experimental analysis of soft fingertips with internal rigid core. In: Proceedings of the 12th International Conference on Advanced Robotics, ICAR 2005, pp. 109–114. IEEE (Year)
4. Dong, R.G., Wu, J.Z.: Analysis of the contact interactions between fingertips and objects with different surface curvatures. Proceedings of the Institution of Mechanical Engineers, Part H: Journal of Engineering in Medicine **219**, 89–103 (2005)
5. Wu, J.Z., Welcome, D.E., Dong, R.G.: Three-dimensional finite element simulations of the mechanical response of the fingertip to static and dynamic compressions. Computer Methods in Biomechanics and Biomedical Engineering **9**, 55–63 (2006)
6. Cabibihan, J.-J., Carrozza, M.C.: Influence of the skin thickness on tactile shape discrimination. In: 2012 4th IEEE RAS & EMBS International Conference on Biomedical Robotics and Biomechatronics (BioRob), pp. 1681–1685. IEEE (Year)
7. Gu, C., Liu, W., Fu, X.: A novel silicon based tactile sensor on elastic steel sheet for prosthetic hand. In: Zhang, X., Liu, H., Chen, Z., Wang, N. (eds.) ICIRA 2014, Part II. LNCS, vol. 8918, pp. 475–483. Springer, Heidelberg (2014)
8. Lee, Y., Hwang, K.: Skin thickness of Korean adults. Surgical and Radiologic Anatomy **24**, 183–189 (2002)
9. Pailler-Mattei, C., Bec, S., Zahouani, H.: In vivo measurements of the elastic mechanical properties of human skin by indentation tests. Medical Engineering & Physics **30**, 599–606 (2008)
10. Jones, L.A., Lederman, S.J.: Human hand function. Oxford University Press (2006)
11. Schneider, F., Draheim, J., Kamberger, R., Wallrabe, U.: Process and material properties of polydimethylsiloxane (PDMS) for Optical MEMS. Sensors and Actuators A: Physical **151**, 95–99 (2009)